Brain Stimulation 14 (2021) 1307–1316

Contents lists available at ScienceDirect

Brain Stimulation

journal homepage: http://www.journals.elsevier.com/brain-stimulation

# An insight into electrical resistivity of white matter and brain tumors

Tammam Abboud [a, *], Günter Hahn [b], Anita Just [b], Mihika Paidhungat [a], Angelina Nazarenus [a], Dorothee Mielke [a], Veit Rohde [a]

[a] Department of Neurosurgery, University Medical Center Göttingen, Robert-Koch-Straße 40, 37075, Göttingen, Germany
[b] Department of Anesthesiology, EIT Research Unit, University Medical Center Göttingen, Robert-Koch-Straße 40, 37075, Göttingen, Germany

ARTICLE INFO

*Article history:*
Received 21 April 2021
Received in revised form
27 August 2021
Accepted 31 August 2021
Available online 1 September 2021

*Keywords:*
Electrical resistivity
Tissue impedance
White matter
Glioma
Metastasis

ABSTRACT

*Background:* There is a lack of information regarding electrical properties of white matter and brain tumors.
*Objective:* To investigate the feasibility of in-vivo measurement of electrical resistivity during brain surgery and establish a better understanding of the resistivity patterns of brain tumors in correlation to the white matter.
*Methods:* A bipolar probe was used to measure electrical resistivity during surgery in a prospective cohort of patients with brain tumors. For impedance measurement, the probe applied a constant current of 0.7 μA with a frequency of 140 Hz. The measurement was performed in the white matter within and outside peritumoral edema as well as in non-enhancing, enhancing and necrotic tumor areas. Resistivity values expressed in ohmmeter (Ω*m) were compared between different intracranial tissues and brain tumors.
*Results:* Ninety-two patients (gliomas WHO II:16, WHO III:10, WHO IV:33, metastasis:33) were included. White matter outside peritumoral edema had higher resistivity values (13.3 ± 1.7 Ω*m) than within peritumoral edema (8.5 ± 1.6 Ω*m), and both had higher values than brain tumors including non-enhancing (WHO II:6.4 ± 1.3 Ω*m, WHO III:6.3 ± 0.9 Ω*m), enhancing (WHO IV:5 ± 1 Ω*m, metastasis:5.4 ± 1.3 Ω*m) and necrotic tumor areas (WHO IV:3.9 ± 1.1 Ω*m, metastasis:4.3 ± 1.3 Ω*m), p=<0.001. No difference was found between low-grade and anaplastic gliomas, p = 0.808, while resistivity values in both were higher than the highest values found in glioblastomas, p = 0.003 and p = 0.004, respectively.
*Conclusions:* The technique we applied enabled us to measure electrical resistivity of white matter and brain tumors in-vivo presumably with a significant effect with regard to dielectric polarization. Our results suggest that there are significant differences within different areas and subtypes of brain tumors and that white matter exhibits higher electrical resistivity than brain tumors.


## 1. Introduction

Brain tumors have proved challenging to treat [1]. Therapeutic approaches have largely addressed the biological characteristics of these cancers. Electrical properties of brain tumors are unknown. Research addressing electrical resistivity of brain tumors is lacking, probably due to the fact that to date no appropriate technique for performing in-vivo measurement of electrical resistivity on brain and tumor tissues has been developed, nor have normative values with regard to the resistivity of different brain tissues, including white matter, been established.

Brain stimulation is a basic technique that underlies several diagnostic and therapeutic procedures such as deep brain stimulation, transcranial magnetic stimulation [2], electrical transcranial and direct cortical electrical stimulation [3,4]. Better understanding of the electrical properties of the brain, such as tissue impedance, is

*Abbreviations:* EIT, electrical impedance tomography; MRI, magnetic resonance imaging; ALA, 5-aminolevulinic acid; **CSF**, cerebrospinal fluid; **Ohm**, Ω; **Ohmmeter**, Ω*m; **R**, resistance; **CST**, corticospinal tract.

* Corresponding author.
*E-mail address:* tammam.abboud@med.uni-goettingen.de (T. Abboud).

https://doi.org/10.1016/j.brs.2021.08.023

essential for the further optimization and development of these applications. More in-depth knowledge of how electrical fields from an intracerebral or external source pass through brain tissues is also required within different research areas, such as modeling studies for electroencephalogram and electrical impedance tomography (EIT) [2,5–7].

Measurement of tissue resistivity has been found to be an effective tool in distinguishing benign tissue from tumor tissues [8] and continues to be used in detecting malignancies in case of prostate [8] and breast cancer [9]. In addition, EIT has been used for detection of pathologic conditions like pulmonary air and fluid accumulations [10]. Measurements of brain tissue resistivity have mainly relied on ex-vivo measurement of samples obtained during surgical treatment of cranial diseases [11]. This approach is technically and ethically practical. Results obtained in this way do not, however, necessarily reflect the real in-vivo resistivity values and differences between intracranial tissues, as cell death commences immediately upon tissue excision leading to an increase in tissue resistivity [12]. In addition, this resistivity is considerably affected by the loss of blood perfusion [13], which occurs as soon as the tissues are extracted. The most common approach for in-vivo impedance measurement is EIT even though this approach has significant limitations, since the scalp and skull diminish the amplitude of the signal [14]. In addition, the amount of current passing through the brain is presumably too miniscule compared to the current shunted by the scalp, thus causing the sensitivity to resistivity differences within the brain to be insufficient [15].

During surgical resection of brain tumors, cancerous tissues can often be recognized due to their special consistency, vasculature and water content. We, therefore, presumed that different areas and subtypes of brain tumors have different electrical resistivity values that might differentiate them from surrounding white matter. To test this hypothesis, we used a bipolar probe — approved for brain stimulation— to measure in-vivo the electrical resistivity of intracranial tissue and brain tumors during surgical resection in a prospective cohort of patients operated for brain tumors. Our intention was to investigate the feasibility of this technique and to establish an understanding of the resistivity patterns of brain tumors in correlation to the white matter.

## 2. Materials and methods

### 2.1. Patient population

All patients who were admitted to our institute between January 2018 and January 2020 for operative treatment of a brain tumor were screened for this study. Most of them were from the southern part of Lower Saxony in Germany. Anyone over the age of 18, regardless of gender, was considered eligible for the study if they had either been diagnosed as having or were suspected of having a glioma or brain metastasis. Only those patients were admitted to the study whose preoperative magnetic resonance imaging (MRI) revealed a tumor of at least 2.5 cm in diameter which was subsequently confirmed via an intraoperative frozen section. Ultimately, the sample size was determined by the number of admissions and the availability of a sole measurement device during the course of the study period. During the operation patients were put in either a supine or sitting position. Intraoperative navigation was performed to plan the surgical approach and to confirm the localization of the measurement probe in the surgical field. Prior to surgery patients with suspected anaplastic gliomas, glioblastomas and brain metastases received 5ALA (5-aminolevulinic acid) prior to the surgery, which was used to make malignant tissue clearly visible during tumor resection.

### 2.2. Anesthesia

All procedures were performed under general intravenous anesthesia. The same protocol was followed for all patients using identical drugs in weight-adjusted doses. Anesthesia was induced and maintained with propofol, analgesia was applied with sufentanil during intubation and continued with remifentanil. Invasive measurement of blood pressure was performed during all procedures to maintain stable systolic and mean blood pressure. Body temperature was maintained at a near normal level.

### 2.3. Technical setup

Measurement of tissue impedance was performed using a bipolar probe with two identical spherical tips (Dr. Langer Medical GmbH; diameter of each sphere = 1.25 mm; distance between the spheres = 5 mm; the spheres are made of medical steel, Fig. 1). This probe has been approved for electrical stimulation of the cortex and white matter during brain surgery. The probe was connected to a device that is used for intraoperative neuromonitoring (ISIS, inomed Medizintechnik GmbH, Germany). To measure the impedance, this device produces a constant current of 0.7 μA at a frequency of 140 Hz. Impedance can be measured in a range between 0 and 500 kΩ with a resolution of 0.1 kΩ. The whole measurement system was checked and calibrated by connecting a series of metal film resistors with a 1% degree of accuracy directly to the tips of the probe. This calibration procedure was performed in the range of 0.1 kΩ–12 kΩ.

### 2.4. Surgery and measurement of tissue impedance

After skin incision, a navigation-guided craniotomy was performed and the dura was exposed. After opening the dura, a cortectomy was conducted and the impedance in the exposed solid tumor tissue was measured. Various tumor areas were measured, depending on the morphological features of the tumor shown on MRI. In metastases and glioblastomas measurement was performed within necrotic and enhancing tumor areas. In grade III gliomas it was done in enhancing and non-enhancing tumor areas while in low-grade gliomas this was carried out in non-enhancing tumor areas. When possible, impedance measurement was also performed in the areas of peritumoral edema and in healthy exposed white matter. These areas were identified through intraoperative navigation, through tissue texture during resection and through the absence of 5ALA enhancement. We performed one measurement for each tissue per patient. During measurement within a tumor or white matter, spherical tips were inserted half way into the tissue and the probe was held in a vertical position with respect to the

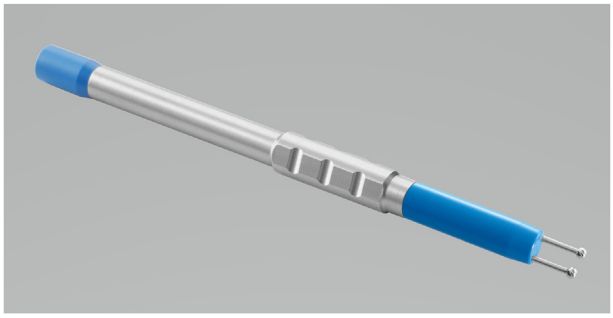

**Fig. 1.** The measurement tool, a bipolar probe with two spherical tips (made of medical steel) which is applied in exposed tumor tissues and white matter. Diameter of each sphere = 1.25 mm and the distance between the spheres = 5 mm.

exposed tissue until the indicated value remained unchanged, which took up to 30 s per measurement. To avoid impurities during measurement, the tissues were kept free of blood and cerebrospinal fluid (CSF) through surgical suction. When fluids appeared to affect the measurement, the procedure was repeated after fluid removal; otherwise, the result was not considered. To avoid interfering with the impedance measurement, other instruments connected to the power supply were not activated during this procedure. Location of the measurement probe was verified for each measurement via neuronavigation to avoid involving more than one tissue type. Impedance values were recorded by a technical assistant and the surgeon performing the measurement could not access the results. Impedance values were expressed in ohm (Ω). Examples of the tumor areas, in which impedance measurements were performed are displayed in images derived from screen shots taken by the navigation system during surgical resection of the tumors (Figs. 2 and 3 and Supplementary Fig. 1).

### 2.5. Estimation of resistivity

To calculate resistivity of the tissues from the resistance measured, the geometry of the measuring arrangement must also be considered. The resistance R, which is equal to the quotient of voltage and current (Ohm's law), depends on the resistivity of the medium ρ and the geometrical factor k:

$$R = \rho * \frac{1}{k} \quad (1)$$

To calculate the geometrical factor with respect to the two spherical tips, a numerical simulation of current injection via two spheres embedded half way in a homogeneous medium with a conductivity of 1 S/m (resistivity: 1 Ω*m) was performed using COMSOL Multiphysics (COMSOL AB, Stockholm, Sweden). A voltage difference of 2 V between the surfaces of the spheres (voltage +1 V and -1 V at the surfaces) was preset and the resulting current density was calculated. The current amplitude I was calculated from the current density by surface integration in the area of the spheres. As R = U/I, the geometrical factor can be calculated then by rearranging (1) into

$$k = \frac{\rho * I}{U} \quad (2)$$

(ρ - resistivity = 1 Ω*m, U – voltage difference = 2 V, Fig. 4A and B).

A verification of the geometrical factor was performed using a conductivity calibration solution (KCl solution, resistivity of 67 Ω*m at 25 °C, Sensortechnik Meinsberg GbmH). This solution with high resistivity was chosen to overcome possible dielectric polarization. At room temperature, the probe was held vertically, the spherical tips of the probe were embedded half way in the solution and the resistivity was measured in a frequency range of 100 Hz–10,000 Hz, using an HP4194A Impedance/Gain-Phase Analyzer.

To estimate the possible effect of dielectric polarization, the measurement was repeated using a conductivity calibration solution with low resistivity (KCl solution, resistivity of 7 Ω*m at 25 °C, Sensortechnik Meinsberg GbmH).

### 2.6. Ethics statement

Approval by the local ethics committee (14/10/2017) was obtained and archived in accordance with local and institutional laws and data protection regulations. This study was performed in accordance with the ethical standards provided in the 1964 Declaration of Helsinki and its later amendments. Informed consent was obtained from the participants prior to surgery.

### 2.7. Statistical analysis

This is an exploratory study, both prospective and observational in nature, a) to determine the feasibility of in-vivo intracranial impedance measurement, b) to investigate whether white matter and different tumor regions have distinct resistivity values, and c) to compare resistivity values among a variety of brain tumors.

For all tests, a p-value less than 0.05 was considered significant. Statistical analysis and graphics were performed using Microsoft Excel (2013, Microsoft Inc, Seattle, Washington, USA), SigmaPlot (v12.5, Systat Software Inc, Erkrath, Germany) and Prism (v9.1.2, GraphPad Software, San Diego, USA). A paired *t*-test was applied to compare resistivity values between different intracranial tissues. We used thew *t*-test to compare resistivity values between the different tumor groups.

### 2.8. Data availability

The anonymized data supporting the findings of this study are available upon request from the corresponding author.

## 3. Results

During the recruitment period 150 patients were screened for the study. Preoperative MRI revealed a suspected meningioma in 15 patients and an inflammation or ischemia in 14 patients, thus leaving 121 eligible patients. Since 19 in this group refused to participate and another 10 had to be because after intraoperative frozen sections exhibited a pathology differing from that of a tumor, we ultimately included 92 patients in the study. They had a mean age of 60 (range 18–88 years); 57% of them were male and 43% were female. Thirty-three patients (40.7%) had a glioblastoma, 33 (29.6%) had a metastasis, 10 (12.3%) had an anaplastic glioma and 16

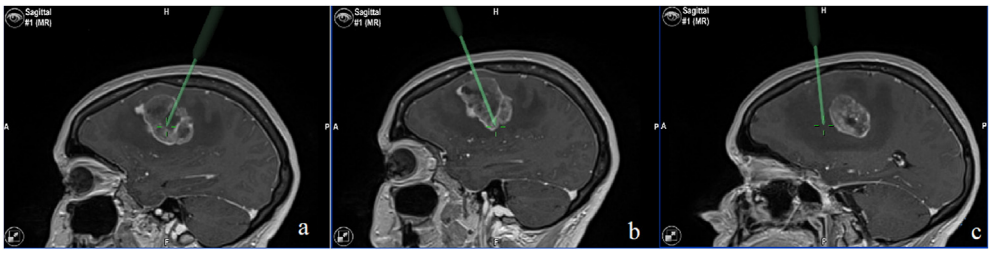


**Fig. 2.** MRI of a patient with glioblastoma. The images were derived from an intraoperative navigation system and show the necrotic (a) and the enhancing tumor areas (b), in which the measurements were performed. The corresponding resistivity values = 2.8 and 4.5 Ω*m, respectively. The measurement was also performed in the peritumoral edema (c). The calculated resistivity value = 8.3 Ω*m.

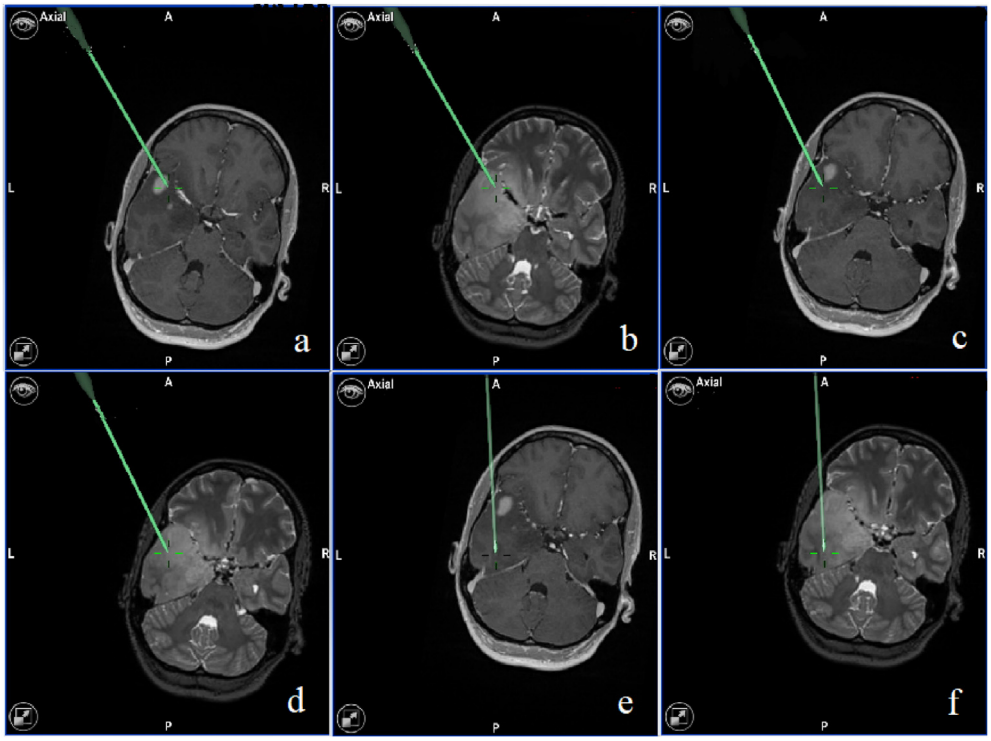


**Fig. 3.** MRI of a patient with anaplastic glioma. The images show different spots, at which the measurements were performed. T1 weighted image (a) and T2 weighted image (b) refer to the same spot within the enhancing part of the tumor with a resistivity value of 4.5 Ω*m. T1 weighted image (c) and T2 weighted image (d) demonstrate a measurement spot within the non-enhancing part of the tumor with a resistivity value of 7.4 Ω*m. T1 weighted image (c) and T2 weighted image (d) show a measurement spot within the white matter with a resistivity value of 12.3 Ω*m.

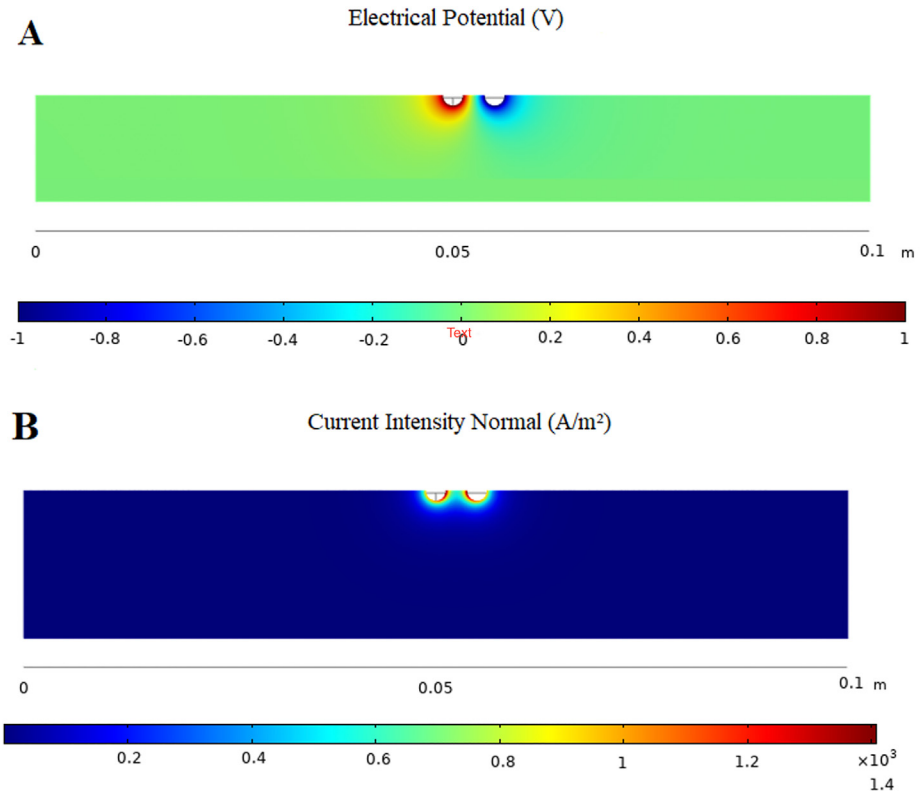


**Fig. 4.** Calculation of the geometrical factor of the probe **A)** Potential distribution, **B)** Distribution of current intensity when the spheres are half embedded in the homogeneous medium with a conductivity of 1 S/m (resistivity: 1 Ω*m), (when voltage difference is set to 2 V between the surfaces of the spheres).

(17.3%) had a low-grade glioma. In 44.4% of the cases the lesions were located in the frontal lobe, in 22.2% in the parietal lobe, in 16%, in the temporal lobe, in 8.6% in the occipital lobe, and in 8.6% in the insula. Nine patients (11.1%) had a recurrent tumor.

### 3.1. Impedance measurements

We analyzed four different subgroups of tumors (low-grade glioma, anaplastic glioma, glioblastoma and metastasis) and two different brain areas (white matter and edema). In three of the four different tumor subgroups (metastases, glioblastomas, and anaplastic glioma) two distinct tumor areas were investigated: contrast-enhancing and necrotic. Measurement was done in 32 patients in contrast-enhancing tumor areas (15 with metastases, 15 with glioblastomas and 2 with anaplastic gliomas). Necrotic tumor areas were measured in 63 patients (32 with glioblastomas and 31 with metastases). Bleeding at the intended measurement site prohibited appropriate measuring in contrast-enhancing tumor areas in 36 patients (18 with metastases, 18 with glioblastomas) and in necrotic tumor areas in 3 patients (1 with glioblastoma and 2 with metastases).

Impedance of non-enhancing tumor areas was measured in all patients with low-grade and anaplastic glioma.

Impedance of white matter within and outside of the peritumoral edema was measured in 32 patients (10 with metastasis, 10 with glioblastoma, 2 with anaplastic glioma and 10 with low-grade glioma). In the remaining patients, a measurement was not performed in the white matter because the tumor resection was not complete, or because hemostasis prohibited the measurement at the conclusion of tumor resection. All measurements were performed at body temperature (37 °C).

Table 1 depicts the number of preformed measurements for each tissue type.

### 3.2. Calibration and geometrical calculation

The whole measurement system displayed a high degree of stability and linearity from 0.1 kΩ to 12 kΩ. The fitted linear calibration curve was

$$R_{measured} = a*R_{set} + b \quad (3)$$

with a = 0.924 und b = 0.0099 kΩ.

$R_{measured}$ denotes the displayed values of resistance and $R_{set}$ denotes the calibration resistors. The latter corresponds to R (resistance) as later used in the tissue measurements. Coefficient of determination ($r^2$) was 0.9998 (Fig. 5).

The numerical simulation yielded a geometrical factor of k = 5.2 mm (spherical tips half embedded). Resistivity ρ (Ω*m) was finally calculated from $R_{measured}$ (kΩ) as follows:

$$\rho = (R_{measured} - b)/a*k. \quad (4)$$

Measurements in the conductivity calibration solution with high resistivity (67 Ω*m) revealed a frequency dependent deviation from the indicated resistivity value of the producer with a mean of −8.6% ± 3.3%. At a frequency of 141 Hz the deviation was as low as 2.2% and the calculated geometrical factor was therefore accepted (Supplementary Table 1).

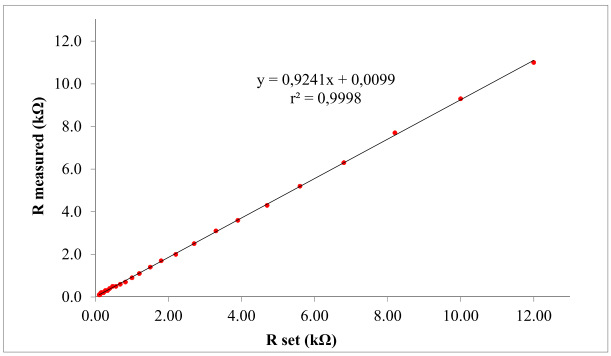


**Fig. 5.** A diagram depicting results of calibration of the measurement device. The whole measurement system showed good stability and linearity in the range of 0.1 kΩ–12 kΩ. The fitted linear calibration curve was $R_{measured} = a*R_{set} + b$ with a = 0.924 und b = 0.0099 kΩ. $R_{measured}$ denotes the displayed values of resistance and $R_{set}$ denotes the calibration resistors. The latter corresponds to R (resistance) as used in the tissue measurements. Coefficient of determination ($r^2$) was 0.9998.

The measurement in the conductivity calibration solution with low resistivity (7 Ω*m) showed a frequency dependent deviation from the indicated resistivity value of the producer with a mean of 19.2% ± 32.3%. At a frequency of 141 Hz the deviation was as high as 81.3% (Supplementary Table 2).

### 3.3. Tissue resistivities

The mean of resistivity values of white matter outside the peritumoral edema was 13.3 ± 1.7 Ω*m (median 12.9, range 9–18 Ω*m).

The resistivity value of white matter within the peritumoral edema had a mean of 8.5 ± 1.6 Ω*m (median 8.4, range 6.7–10.1 Ω*m).

In patients with low-grade glioma, the mean of the resistivity values was 6.4 ± 1.3 Ω*m (median 6.4, range 4.5–8.4 Ω*m).

In patients with anaplastic gliomas the mean of resistivity values of non-enhancing tumor areas was 6.3 ± 0.9 Ω*m (median 6.1, range 5.6–8.4 Ω*m). Measurements in contrast-enhancing tumor areas were performed in two patients with anaplastic glioma and each displayed a resistivity value of 4.5 Ω*m.

In patients with glioblastoma, the mean of the resistivity values in contrast-enhancing tumor areas was 5 ± 1 Ω*m (median 5, range 3.3–7.3 Ω*m). The mean of the resistivity values in necrotic tumor areas was 3.9 ± 1.1 Ω*m (median 3.9, range 1.6–8.4 Ω*m).

In patients with brain metastases, the mean of the resistivity values in contrast-enhancing tumor areas was 5.4 ± 1.3 Ω*m (median 5.6, range 2.8–7.8 Ω*m), and the mean of the resistivity values in necrotic tumor areas was 4.3 ± 1.3 Ω*m (median 3.9, range 2.2–8.4 Ω*m).

**Table 1**
Number of measurements performed for each tissue subtype.

| | Number of included patients | Non-enhancing area[a] | Enhancing areas[a] | Necrotic areas[a] | White matter (edema)[a] | White matter (outside edema)[a] |
|---|---|---|---|---|---|---|
| Low grade glioma | 16 | 16 | 0 | 0 | 2 | 10 |
| Anaplastic glioma | 10 | 10 | 2 | 0 | 2 | 2 |
| Glioblastoma | 33 | 0 | 15 | 32 | 5 | 10 |
| Metastasis | 33 | 0 | 15 | 31 | 5 | 10 |
| Total (patients) | 92 | 26 | 32 | 63 | 14 | 32 |

[a] Number of patients, in whom the measurement was performed in this area.

When all tumors were considered together, the mean of resistivity values of necrotic tumor areas was 4 ± 1.2 Ω*m (median 3.9, range 1.6–8.3 Ω*m). The mean of resistivity values of enhancing tumor areas was 5.1 ± 1.7 Ω*m (median 5 Ω*m, range 2.8–7.8 Ω*m). The mean of resistivity values of non-enhancing tumor areas was 6.3 ± 1.1 Ω*m (median 6.1, range 4.5–8.4 Ω*m).

### 3.4. Analysis

White matter outside peritumoral edema had higher resistivity values than did white matter within peritumoral edema; and both had higher resistivity values than brain tumors, including non-enhancing, enhancing and necrotic brain areas (paired *t*-test, p = <0.001, Fig. 6A). There was no correlation between age and resistivity values of white matter (p = 0.245).

No overlap was found between resistivity values of brain and tumor tissues stemming from the same patient. Resistivity of white matter was on average 158% higher than the highest tumor values (range 54%–346%). Resistivity of edema was on average 85% higher than the highest tumor values (range 15%–204%). Resistivity of white matter was on average 60% higher than resistivity of edema (range 24%–114%).

The tumor groups studied were not significantly different regarding gender or age (chi-squared test p = 0.823 and p = 0.689, respectively). Resistivity values within contrast-enhancing tumor areas in glioblastomas were higher in comparison to those in necrotic tumor areas (paired *t*-test p = <0.001, Fig. 6B). The same result was found in metastases with significantly higher values in contrast-enhancing tumor areas (paired *t*-test p = <0.001, Fig. 6B). No significant difference in resistivity values was found between glioblastomas and metastases when comparing necrotic tumor areas or contrast-enhancing tumor areas in both tumor groups (*t*-test p = 0.193 and p = 0.334, respectively, Fig. 6B).

No difference in resistivity values was found between low-grade and anaplastic gliomas (*t*-test p = 0.808), whereas resistivity values in both were higher than the highest values found in glioblastomas (*t*-test p = 0.003 and p = 0.004, respectively, Fig. 6C).

When all tumors were considered together, values of necrotic tumor areas were lower than those of enhancing tumor areas and both were lower than those of non-enhancing areas (t-rest p = <0.001, Fig. 6D).

## 4. Discussion

In this study, we evaluated a technique for non-invasive in-vivo measurement of electrical resistivity of intracranial tissues and brain tumors using a bipolar probe. This technique was feasible during surgical resection of brain tumors and allowed us to approach electrical characteristics of intracranial tissues and brain tumors. Although a systematic error in the absolute resistivity may exist, we found distinct resistivity values for white matter within and outside of peritumoral edema which were higher than the resistivity values of tumor tissues. Glioblastomas and metastases were not homogenous in their electrical resistivity. We found a significant difference between necrotic and contrast-enhancing tumor areas; moreover, resistivity values in metastases and glioblastomas were lower than those in less malignant tumors including low-grade and anaplastic gliomas. A certain overlap in the range of resistivity values was found between contrast-enhancing and low-grade gliomas as well as between white matter within peritumoral edema and low-grade gliomas. The range of resistivity of healthy white matter did not overlap with that of other tissues. The aforementioned overlap might be attributed to differences among patients, since such an overlap was not found between the brain and tumor tissues from individual patients. Another explanation for the observed variation might be found in the conditions in which the measurements were performed. A computational study during electrical subcortical stimulation suggested, for example, that bipolar stimulation might be subjective to variations in moisture conditions [16]. In the current study we always kept the measurement site dry; however, we cannot rule out the existence of an invisible fluid layer which could have contributed to the variations seen in the measured values.

To date intracranial in-vivo measurement of brain tissue resistivity has only been described twice in the literature. Although Latikka et al. did not utilize a statistical analysis – probably due to the small number of patients–, they paved the way by performing such measurements with a monopolar needle electrode in nine patients during brain surgery. Mean resistivity values were 3.5 Ω*m for grey matter and 3.9 Ω*m for white matter; values for tumor tissues ranged from 2.3 to 9.7 Ω*m [17]. The second group to report on measurements of brain tissue resistivity was Koessler et al.. In a sterotactic procedure performed on 15 epileptic patients, they used intracerebral multi-contact electrodes designed for stereo-electroencephalography and noted mean resistivity values of 3.8 Ω*m for grey matter, 5.2 Ω*m for white matter and 3.5 Ω*m for the epileptogenic zones. They reported a statistically significant difference between healthy grey and white matter; grey matter had a higher resistivity in healthy tissue than in epileptogenic zones [5].

In a meta-analysis of the data from 15 studies on electrical conductivities in human head tissue, McCann et al. found that values varied significantly depending on the method and frequency. They cited measurements performed using either EIT, magnetic resonance EIT, electro- or magnetoencephalography, diffusion tensor imaging (DTI) or directly applied current in-vitro/ex-vivo. The mean value for white matter was 4.2 Ω m with a range of 1.2–15.5 Ω m. Our method implemented a directly applied current in-vivo. This fact limits the comparability of our data with data from previous studies which adhered to a different measurement principle such as EIT or DTI or which collected measurements in-vitro or ex-vivo under different conditions [18]. The data presented by Latikka et al. and Koessler et al. recorded the resistivity of white matter to be 3.9 Ω m and 5.2 Ω m, respectively. Since they carried out their measurements using current directly applied in-vivo, we can make reliable comparisons between their data and ours. Given that both studies applied a frequency of 50 kHz, higher resistivity values of white matter were expected at lower frequencies, as observed in our study (at 140 Hz resistivity = 13.3 ± 1.7 Ω m). We expected this, because resistivity of human tissues is frequency dependent and it increases at lower frequencies [19]. The absolute values of tissue resistivity seem to differ according to the measurement method, whereby the relationship between resistivity values of healthy and pathological tissues within the brain measured with the same method and frequency should not be affected.

### 4.1. Dielectric polarization

Dielectric polarization might also offer further explanation of why resistivity values in our studies were higher. To estimate the effect of dielectric polarization, we performed the measurement in a low resistivity solution (7 Ω m) and found a deviation of 81.3% (Supplementary Table 2), suggesting that dielectric polarization might have led to higher resistivity values by a factor of approx. 1.8. Such a factor would explain the difference between our values and those measured by Latikka et al. and Koessler et al. We have to take into consideration that neither of their studies investigated the role of the dielectric polarization, and that dielectric polarization is usually affected by a wide variety of factors. It has been reported that dielectric polarization can depend upon the topography of the electrode surface and its area on a microscopic level, as well as

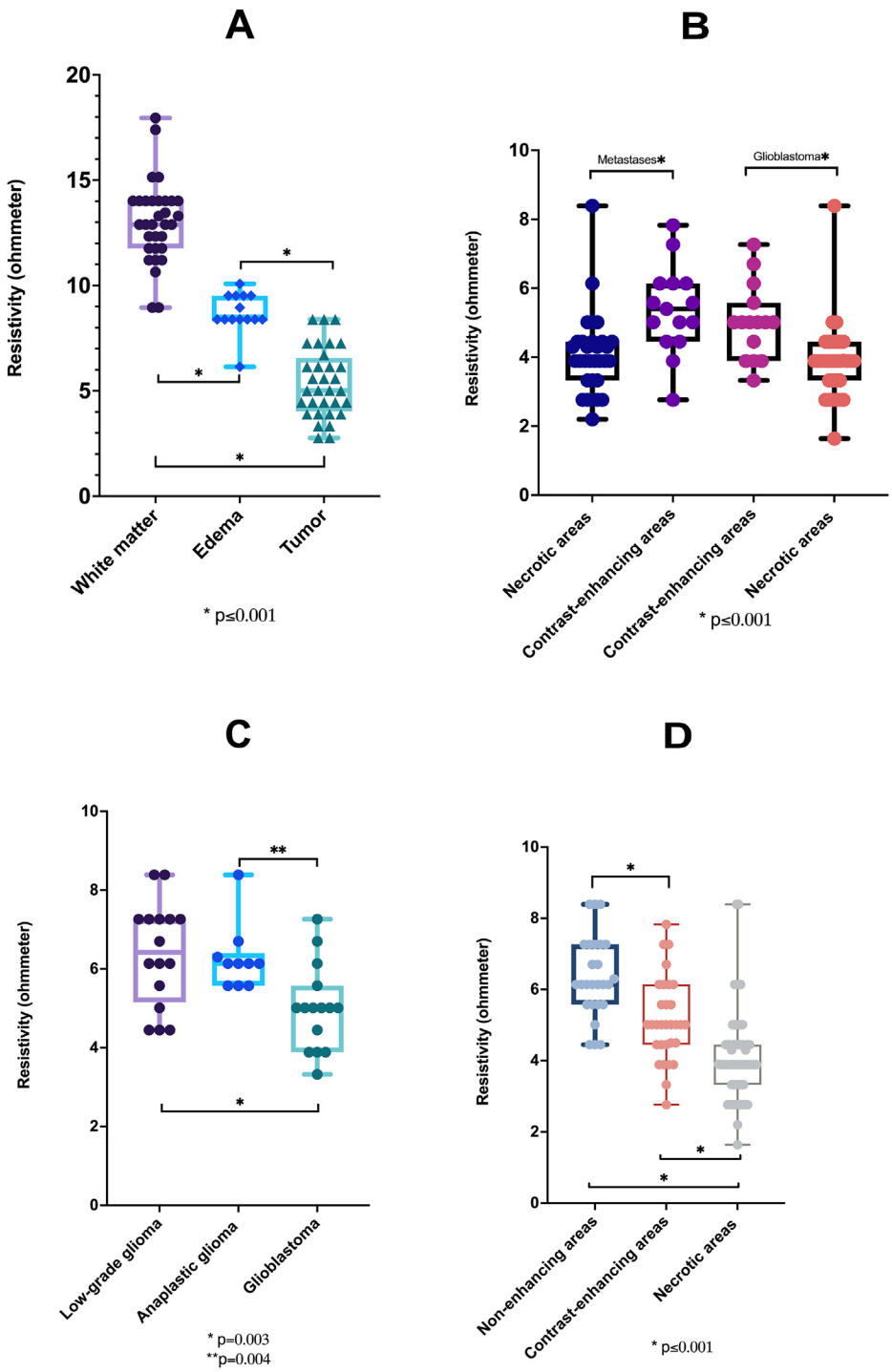


**Fig. 6.** Boxplots showing, **A)** resistivity values of white matter compared to tumor tissues: White matter outside peritumoral edema had higher resistivity values than white matter within peritumoral edema, and both had higher resistivity values than brain tumors including non-enhancing, enhancing and necrotic brain areas, paired *t*-test, p = <0.001, **B)** resistivity values of necrotic and contrast-enhancing tumor areas in glioblastomas and metastases: In both, resistivity values within contrast-enhancing tumor areas were higher in comparison to those in necrotic tumor areas, paired *t*-test p = <0.001, **C)** resistivity values of different gliomas (glioblastomas are represented by their highest resistivity values): No difference in resistivity values was found between low-grade and anaplastic gliomas, *t*-test p = 0.808. Resistivity values in low-grade and anaplastic gliomas were higher than the highest values found in glioblastomas (contrast-enhancing tumor areas), *t*-test p = 0.003 and p = 0.004, respectively, **D)** resistivity values of all tumors: Values of necrotic tumor areas were lower than those of enhancing tumor areas and both were lower than those of non-enhancing areas, *t*-test p = <0.001.

upon the surface chemistry or the electrode/sample interface. Because of the fact that these effects can be so very diverse, no simple correction technique has been widely accepted [3]. For this reason, we did not undertake a correction of the resistivity values, which would have been dependent on the estimated polarization effect. Instead, we accepted the possibility of a systematic error and tried to quantify the resistivity as a whole to detect the differences between the various tissues.

### 4.2. Electrical anisotropy

A certain variability in the resistivity values of white matter was expected, since electrical conductivity of brain tissue, particularly white matter, is known to be anisotropic. In our current study, it was not possible to plan in advance as to whether the actual measurement angle would be longitudinal or across the fibers because that was ultimately dictated by the surgical approach itself. Electrical anisotropy of white matter was investigated during in-vivo animal experiments [20,21]. Nicholson has reported on the anisotropy of white matter (cat internal capsule, in-vivo) and suggested a factor of between 9 and 10 for the conductivity along and across the fibers [21,22]. That anisotropy has an effect on the conductivity of white matter has not yet been studied in-vivo on human brain tissue. Anisotropic conductivity profiles of the human brain have, in most cases, been derived from diffusion weighted MRI [6,23]. Although it is possible to measure fractional anisotropy using DTI, the range within which the recorded values would affect results of electrical impedance measurement remains unknown. Our random measurement in white matter showing a lack of a high impact of anisotropy mirrors results from a study done with dipolar electrical sources and intracranial measurement using intracranial electrodes. In that study a better prediction with a model containing CSF and brain anisotropy (based on DTI) was shown and the model with a global anisotropic ratio of 10:1 between the eigenvalues (parallel: tangential to the fiber direction) had the poorest performance of all the anisotropic models [24].

### 4.3. A different approach of understanding brain tumors

Our data suggest that healthy intracranial tissues have different resistivity values than do tumorous tissues. Even peritumoral edema showed distinct resistivity values that were higher than those of tumor tissue. These findings are in accordance with the literature available on resistivity values of extracranial cancer tissues known to have lower resistivity values than the surrounding healthy tissues [25,26]. Ex-vivo studies on extra-cranial tumor tissues have already shown that malignant tissues have a lower resistivity at a variety of frequencies due mainly to water content, which increases in malignant tissues [27,28]. An ex-vivo study found that the permittivity and conductivity were 30% higher in tumors than in the surrounding tissues due to their higher water content [29]. This concurs with our results. Our measurements applied a single low frequency and provided in-vivo assessment of brain tissue and tumors under sustained blood perfusion. Our findings are also supported by the well-known fact that blood perfusion increases with malignancy [30]. Using electron microscopy Bakay et al. measured the extracellular spaces in 15 human intracranial tumors. They found that these extracellular spaces were enlarged in each of the gliomas examined. In most of these tumors the extracellular space was enlarged on average by 20–40%. The average size of the normal extracellular white matter was calculated at 6–7% [31]. These findings suggest that there is a correlation between the enlargement of extracellular space found in gliomas and the fact that tumor as well as peritumoral edema had lower resistivity values than did white matter.

Although it is possible to study electrical properties of tumor tissues using MRI [32,33], this approach is limited in its clinical applicability. When optimized for a clinical setting, its use is limited to diagnostics and treatment monitoring (follow-up) [34]. Direct intraoperative measurement could lead to a real time recognition of pathological tissue during surgery. This would thus support all other methods used to distinguish pathological tissue from normal tissue.

During surgical resection of brain tumors, areas of different consistencies are usually encountered. We performed the measurement in various areas of the tumor and obtained different resistivity values. This is a finding we expected as brain tumors in general and metastasis and glioblastomas in particular are known to be inhomogeneous. In addition, low-grade and anaplastic glioma displayed higher resistivity values than did the more malignant tissue of glioblastoma, which is known to exhibit necrosis as an important biological feature compared to WHO I, II, and III gliomas [35]. One can imagine a resistivity model (Fig. 7) in which tissue resistivity values decrease, the more pathological or tumorous the tissue becomes (Fig. 3). Such a model can, when further validated, be the basis of resistivity-guided tumor resection. Since, in the current study, we were not able to investigate all relevant tumor areas such as the zone in glioblastomas directly outside enhancing areas, we believe that each and every tumor area should undergo a screening for electrical resistivity prior to any possible clinical application.

Because MRI-based diagnoses of brain tumors are so reliable, there is no diagnostic need for the use of impedance measurement, as is often the case in other cancers such as breast and prostate cancer. Image-guided tumor resection has now been the standard for decades; nevertheless, the discrepancy between the extent of intended tumor resection and the de facto extent of tumor resection as confirmed in postoperative imaging is still considered to be a serious neuro-oncological issue [36]. A tool for resistivity-guided tumor resection could be a significant and useful addition to the surgical techniques currently available.

Data with respect to significant differences in the elasticity between normal brain tissue and brain tumors are already available in the literature [37]. Whereas we would expect a correlation between elasticity and electrical conductivity of brain tissues and tumors, an investigation of this issue did not lie within the scope of our study. It could, however, be addressed in the future.

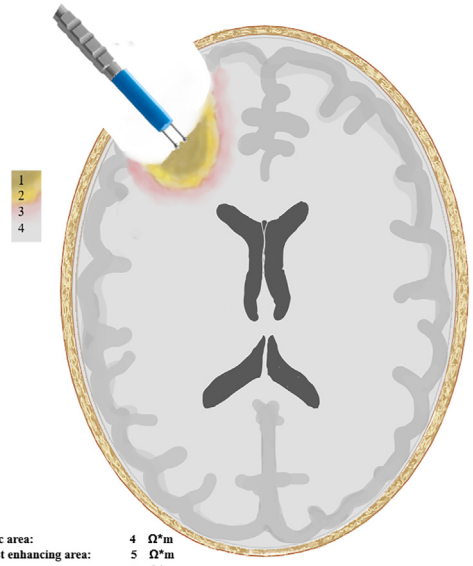


**Fig. 7.** Schematic drawing of the measurement procedure during surgery for a brain tumor. The different colors represent the various areas within the tumor as well as peritumoral edema and white matter with their corresponding average resistivity values. (For interpretation of the references to color in this figure legend, the reader is referred to the Web version of this article.)

### 4.4. Subcortical stimulation and tissue resistivity

The use of electrical cortical and subcortical stimulation as a mapping method to detect the corticospinal tract (CST) has been established over the past few decades [38–40]. Tumor resection under continuous monopolar subcortical stimulation was developed as a means of decreasing the possibility of damaging the CST [4]. A threshold of 5 mA intensity, at which a muscle action potential can be evoked, was considered to be a safe point to stop tumor resection without causing mechanical damage to the CST [41]. A correlation between the intensity of the stimulating current and the distance between the stimulation site and CST has been suggested in many studies. One study based on intraoperative image analysis found a linear correlation between the current intensity and the distance to the CST and estimated this correlation to be approximately 0.97 mA per 1 mm distance to the CST [42]. Another group used titanium clips to mark stimulation sites and a postoperative MRI to estimate this distance. They did not find a linear correlation between the current intensity and the distance to the CST, for the CST was reached sooner than a linear correlation would have projected [43]. Others estimated the correlation at 1.8 mA per 1 mm [44]. What these studies have in common is that the analysis of the correlation between electrical stimulation and the distance to the CST included a variety of different pathologies and assumed a constant electrical resistivity [43]. Our results indicate that there is a difference in the resistivity values between white matter and brain tumors; moreover, brain tumors showed inhomogeneity in resistivity values within the tumor itself and in relation to the tumor subtype as well. Thus, the current passing through these tissues encounters varying resistivity values. This might be an explanation for the discrepancy found in the studies mentioned above with regard to the correlation between the distance to the CST and current intensity. Our results reveal that a reevaluation of this correlation is necessary and that the resistivity value of each tumor must be considered separately.

### 4.5. Limitations and areas of further research

As a criticism of our methodology, one could note that the measurement was performed at particular spots within the tumor or the white matter. A screening of the electrical resistivity of as many spots as possible would be requisite to attain a comprehensive picture of the electrical resistivity of the tumor within the white matter. This would then be similar to the images generated by EIT. The technical apparatus for such an in-vivo screening is not available at the moment but could be the focus of further research. Our measurements were done at a low frequency, thus giving the electrical property of the extracellular liquid a decisive role in the impedance measurement. Cell membranes have a high electrical capacity at low frequency, which hardly involves the intracellular compartment in the current conduction. This can change at higher frequencies; under such conditions the current flows equally through the extra- and intracellular space and the impedance measurement reflects the current conductivity and volume of both compartments [45]. Resistivity measurement of brain tumors with high frequencies would be valuable and would most probably enhance the differences between healthy brain tissues and brain tumors found in our study. As discussed earlier, we did not address the effect of electrical anisotropy on impedance measurement within white matter and tumor tissue; this effect could, however, be the focus of additional research. We also have not investigated the resistivity of grey matter within the framework of this study. Since the surface of the exposed cortex is covered by pia mater and arachnoid, a measurement of cortical convexity would have to have included these layers; furthermore, any incision of the cortex leads to the opening of subarachnoid space where direct measurement there would be influenced by CSF.

In this study we measured the resistivity of large tumors whereby white matter was assumed to be an extended area. Thus, in our numerical simulation, we based the calculation of geometric factor on the assumption that we were dealing with a homogeneous medium. As mentioned above, measurements in the skull are not only influenced by the tissue under investigation but also by neighboring structures. Gomez-Tame et al. have, for example, examined the influence of tumor thickness and the CSF layer [16]. Such numerical simulations on realistic head models could possibly be a useful tool in helping to make the interpretation of resistivity measurements in future research more precise.

A final limitation involves 5ALA, which was administered shortly before surgery to make malignant tissue during tumor resection clearly visible. The administration of 5-ALA leads to the accumulation of protoporphyrin IX specifically in cancer cells [46,47]. The effect of such an accumulation on tissue resistivity remains an unknown and was not considered within the framework of our study.

## CRediT authorship contribution statement

**Tammam Abboud:** Conception and design, Methodology, Acquisition of data, Formal analysis, Visualization, Writing – review & editing. **Günter Hahn:** Methodology, Formal analysis, Visualization, Writing – review & editing. **Anita Just:** Methodology, Formal analysis, Visualization, Writing – review & editing. **Mihika Paidhungat:** Formal analysis, Writing – review & editing. **Angelina Nazarenus:** Acquisition of data. **Dorothee Mielke:** Acquisition of data, Writing – review & editing. **Veit Rohde:** Conception and design, Acquisition of data, Writing – review & editing.

## Declaration of competing interest

The authors report no conflict of interest.

## Acknowledgements

We are very grateful to Christina Moosauer-Abboud for her kind assistance with the graphics. We would also like to thank Mr. Thomas Asendorf for his mindful support with the statistics. Of course, we would certainly thank David Starr for helping us to revise this manuscript.

## Appendix A. Supplementary data

Supplementary data to this article can be found online at https://doi.org/10.1016/j.brs.2021.08.023.

## Funding

The authors received no funding for this study.

## References

[1] Aldape K, Brindle KM, Chesler L, Chopra R, Gajjar A, Gilbert MR, et al. Challenges to curing primary brain tumours. Nat Rev Clin Oncol 2019;16(8):509–20.
[2] Wagner T, Eden U, Rushmore J, Russo CJ, Dipietro L, Fregni F, et al. Impact of brain tissue filtering on neurostimulation fields: a modeling study. Neuroimage 2014;85(Pt 3):1048–57.
[3] Abboud T, Schaper M, Dührsen L, Schwarz C, Schmidt NO, Westphal M, et al. A novel threshold criterion in transcranial motor evoked potentials during surgery for gliomas close to the motor pathway. J Neurosurg 2016;125(4):795–802.

[4] Raabe A, Beck J, Schucht P, Seidel K. Continuous dynamic mapping of the corticospinal tract during surgery of motor eloquent brain tumors: evaluation of a new method. J Neurosurg 2014;120(5):1015–24.
[5] Koessler L, Colnat-Coulbois S, Cecchin T, Hofmanis J, Dmochowski JP, Norcia AM, et al. In-vivo measurements of human brain tissue conductivity using focal electrical current injection through intracerebral multicontact electrodes. Hum Brain Mapp 2017;38(2):974–86.
[6] Haueisen J, Tuch DS, Ramon C, Schimpf PH, Wedeen VJ, George JS, et al. The influence of brain tissue anisotropy on human EEG and MEG. Neuroimage 2002;15(1):159–66.
[7] Huang Y, Parra LC, Haufe S. The New York Head—a precise standardized volume conductor model for EEG source localization and tES targeting. Neuroimage 2016;140:150–62.
[8] Khan S, Mahara A, Hyams ES, Schned AR, Halter RJ. Prostate cancer detection using composite impedance metric. IEEE Trans Med Imag 2016;35(12):2513–23.
[9] Campisi MS, Barbre C, Chola A, Cunningham G, Woods V, Viventi J. Breast cancer detection using high-density flexible electrode arrays and electrical impedance tomography. In: Conference proceedings: annual international conference of the IEEE engineering in medicine and biology society IEEE engineering in medicine and biology society annual conference 2014; 2014. p. 1131–4.
[10] Hahn G, Just A, Dudykevych T, Frerichs I, Hinz J, Quintel M, et al. Imaging pathologic pulmonary air and fluid accumulation by functional and absolute EIT. Physiol Meas 2006;27(5):S187–98.
[11] Akhtari M, Bryant HC, Mamelak AN, Flynn ER, Heller L, Shih JJ, et al. Conductivities of three-layer live human skull. Brain Topogr 2002;14(3):151–67.
[12] Akhtari M, Salamon N, Duncan R, Fried I, Mathern GW. Electrical conductivities of the freshly excised cerebral cortex in epilepsy surgery patients; correlation with pathology, seizure duration, and diffusion tensor imaging. Brain Topogr 2006;18(4):281–90.
[13] Nyboer J. Electrical impedance plethysmography; a physical and physiologic approach to peripheral vascular study. Circulation 1950;2(6):811–21.
[14] Koessler L, Cecchin T, Colnat-Coulbois S, Vignal JP, Jonas J, Vespignani H, et al. Catching the invisible: mesial temporal source contribution to simultaneous EEG and SEEG recordings. Brain Topogr 2015;28(1):5–20.
[15] Fabrizi L, Sparkes M, Horesh L, Perez-Juste Abascal JF, McEwan A, Bayford RH, et al. Factors limiting the application of electrical impedance tomography for identification of regional conductivity changes using scalp electrodes during epileptic seizures in humans. Physiol Meas 2006;27(5):S163–74.
[16] Gomez-Tames J, Kutsuna T, Tamura M, Muragaki Y, Hirata A. Intraoperative direct subcortical stimulation: comparison of monopolar and bipolar stimulation. Phys Med Biol 2018;63(22):225013.
[17] Latikka J, Kuurne T, Eskola H. Conductivity of living intracranial tissues. Phys Med Biol 2001;46(6):1611–6.
[18] McCann H, Pisano G, Beltrachini L. Variation in reported human head tissue electrical conductivity values. Brain Topogr 2019;32(5):825–58.
[19] Faes TJ, van der Meij HA, de Munck JC, Heethaar RM. The electric resistivity of human tissues (100 Hz-10 MHz): a meta-analysis of review studies. Physiol Meas 1999;20(4):R1–10.
[20] Geddes LA, Baker LE. The specific resistance of biological material–a compendium of data for the biomedical engineer and physiologist. Med Biol Eng 1967;5(3):271–93.
[21] Nicholson PW. Specific impedance of cerebral white matter. Exp Neurol 1965;13(4):386–401.
[22] Gabriel C, Peyman A, Grant EH. Electrical conductivity of tissue at frequencies below 1 MHz. Phys Med Biol 2009;54(16):4863–78.
[23] Güllmar D, Haueisen J, Reichenbach JR. Influence of anisotropic electrical conductivity in white matter tissue on the EEG/MEG forward and inverse solution. A high-resolution whole head simulation study. Neuroimage 2010;51(1):145–63.
[24] Bangera NB, Schomer DL, Dehghani N, Ulbert I, Cash S, Papavasiliou S, et al. Experimental validation of the influence of white matter anisotropy on the intracranial EEG forward solution. J Comput Neurosci 2010;29(3):371–87.
[25] Hope TA, Iles SE. Technology review: the use of electrical impedance scanning in the detection of breast cancer. Breast Cancer Res 2004;6(2):69–74.
[26] Li Z, Deng G, Li Z, Xin SX, Duan S, Lan M, et al. A large-scale measurement of dielectric properties of normal and malignant colorectal tissues obtained from cancer surgeries at Larmor frequencies. Med Phys 2016;43(11):5991.
[27] Schepps JL, Foster KR. The UHF and microwave dielectric properties of normal and tumour tissues: variation in dielectric properties with tissue water content. Phys Med Biol 1980;25(6):1149–59.
[28] Joines WT, Zhang Y, Li C, Jirtle RL. The measured electrical properties of normal and malignant human tissues from 50 to 900 MHz. Med Phys 1994;21(4):547–50.
[29] Lu Y, Li B, Xu J, Yu J. Dielectric properties of human glioma and surrounding tissue. Int J Hyperther 1992;8(6):755–60.
[30] Jain R. Perfusion CT imaging of brain tumors: an overview. Am J Neuroradiol 2011;32(9):1570.
[31] Bakay L. The extracellular space IN brain tumours: I. Morphological considerations. Brain 1970;93(4):693–8.
[32] Huhndorf M, Stehning C, Rohr A, Helle M, Katscher U, Jansen O. Systematic brain tumor conductivity study with optimized EPT sequence and reconstruction algorithm. 2012.
[33] van Lier AL, Raaijmakers A, Voigt T, Lagendijk JJ, Luijten PR, Katscher U, et al. Electrical properties tomography in the human brain at 1.5, 3, and 7T: a comparison study. Magn Reson Med 2014;71(1):354–63.
[34] Mandija S, Meliadò EF, Huttinga NRF, Luijten PR, van den Berg CAT. Opening a new window on MR-based Electrical Properties Tomography with deep learning. Sci Rep 2019;9(1):8895.
[35] Liu S, Wang Y, Xu K, Wang Z, Fan X, Zhang C, et al. Relationship between necrotic patterns in glioblastoma and patient survival: fractal dimension and lacunarity analyses using magnetic resonance imaging. Sci Rep 2017;7(1):8302.
[36] Black PM, Alexander 3rd E, Martin C, Moriarty T, Nabavi A, Wong TZ, et al. Craniotomy for tumor treatment in an intraoperative magnetic resonance imaging unit. Neurosurgery 1999;45(3):423–31. discussion 31-3.
[37] Chauvet D, Imbault M, Capelle L, Demene C, Mossad M, Karachi C, et al. In vivo measurement of brain tumor elasticity using intraoperative shear wave elastography. Ultraschall der Med 2016;37(6):584–90.
[38] Bello L, Castellano A, Fava E, Casaceli G, Riva M, Scotti G, et al. Intraoperative use of diffusion tensor imaging fiber tractography and subcortical mapping for resection of gliomas: technical considerations. Neurosurg Focus 2010;28(2):E6.
[39] Berger MS, Kincaid J, Ojemann GA, Lettich E. Brain mapping techniques to maximize resection, safety, and seizure control in children with brain tumors. Neurosurgery 1989;25(5):786–92.
[40] Duffau H, Lopes M, Arthuis F, Bitar A, Sichez JP, Van Effenterre R, et al. Contribution of intraoperative electrical stimulations in surgery of low grade gliomas: a comparative study between two series without (1985-96) and with (1996-2003) functional mapping in the same institution. J Neurol Neurosurg Psychiatry 2005;76(6):845–51.
[41] Seidel K, Beck J, Stieglitz L, Schucht P, Raabe A. The warning-sign hierarchy between quantitative subcortical motor mapping and continuous motor evoked potential monitoring during resection of supratentorial brain tumors. J Neurosurg 2013;118(2):287–96.
[42] Nossek E, Korn A, Shahar T, Kanner AA, Yaffe H, Marcovici D, et al. Intraoperative mapping and monitoring of the corticospinal tracts with neurophysiological assessment and 3-dimensional ultrasonography-based navigation. Clinical article. J Neurosurg 2011;114(3):738–46.
[43] Shiban E, Krieg SM, Haller B, Buchmann N, Obermueller T, Boeckh-Behrens T, et al. Intraoperative subcortical motor evoked potential stimulation: how close is the corticospinal tract? J Neurosurg 2015;123(3):711–20.
[44] Kamada K, Todo T, Ota T, Ino K, Masutani Y, Aoki S, et al. The motor-evoked potential threshold evaluated by tractography and electrical stimulation. J Neurosurg 2009;111(4):785–95.
[45] Van Loan MD, Withers P, Matthie J, Mayclin PL. Use of bioimpedance spectroscopy to determine extracellular fluid, intracellular fluid, total body water, and fat-free mass. Basic Life Sci 1993;60:67–70.
[46] Chibazakura T, Toriyabe Y, Fujii H, Takahashi K, Kawakami M, Kuwamura H, et al. 5-Aminolevulinic acid enhances cell death under thermal stress in certain cancer cell lines. Biosci Biotechnol Biochem 2015;79(3):422–31.
[47] [Urgent neurosurgical operations in neurooncology]. Zh Vopr Neirokhir Im N N Burdenko 2011;75(3):62–70. discussion -1.